・成松 久：糖鎖科学の基盤技術開発と、それを利用した肝線維化マーカー、および肝がん、胆管癌マーカーの開発，日東紡セミナー，東京, 2011/11/26

・成松 久：疾患特異的バイオマーカーとしての糖鎖（糖鎖をつかう）, KAST 教育講座： 糖鎖科学・糖鎖工学の基礎から応用 ～糖鎖を知る、見る、創る、使う～, かながわサイエンスパーク(KSP)（川崎市）, 2012/1/25

・成松 久：糖鎖研究の基盤開発からバイオマーカーの実用化、そして国際動向、特にアジア戦略について，平成 23 年度 第 11 回 産総研・産技連 LS-BT 合同研究発表会，産総研 つくばセンター 共用講堂, 2012/1/31

Ⅱ．分担研究報告

４．臨床検体収集体制の構築

研究分担者氏名（所属研究機関名）
溝上雅史、伊藤清顕（国立国際医療研究センター）、八橋弘（長崎医療センター）、坂元亨宇（慶應義塾大学・医学部）、武冨紹信（九州大学、途中で北海道大学に異動）

Ａ．研究体制の構築

上記、1～3 の課題で得られたマーカー候補を測定する検体を収集するため、各機関で倫理委員会の承認を得た。また、他の協力機関にも声をかけ、研究開発を効率よく遂行するための体制作りを行った。協力機関の候補としては、札幌厚生病院、山形大学、東京大学、武蔵野赤十字病院、信州大学、順天堂大学医学部附属静岡病院、大垣市民病院、愛知医科大学、川崎医科大学、愛媛大学、九州大学があり、過去二回の班会議には研究協力者として参加をお願いした。

Ｂ．研究テーマの検討

さらに、マーカーの測定を効率よく行うために、検体をテーマごとに分類し重複を無くすことが重要であると考えられる。また、研究分担者や研究協力者ごとに興味の対象は異なっていため、測定の意味のあるもの、本事業として成果の出易いものから優先順位をつけ、検討を行う必要がある。優先順位は、検体数も加味し、溝上 研究分担者と成松 研究代表者が中心となり決定することとし、まずは各研究者の興味のあるテーマの募集も開始した。なお、平成 24 年 6 月を目途に国立国際医療研究センターで検体の受入れが可能になる。また、平成 24 年度第一回班会議（8 月 24 日を予定）の場で測定結果のディスカッションができるように、テーマ決定、検体送付、匿名化、マーカー（ProteinX）の測定を実施する予定である。

Ⅲ. 研究成果の刊行に関する一覧表

Ⅲ．研究成果の刊行に関する一覧表

雑誌（1/2）

発表者氏名	論文タイトル名	発表誌名	巻号	ページ	出版年
Kuno A, Ikehara Y, Tanaka Y, Saito K, Ito K, Tsuruno C, Nagai S, Takahama Y, Mizokami M, Hirabayashi J, Narimatsu H. （参考）	LecT-Hepa: A triplex lectin-antibody sandwich immune-assay for estimating the progression dynamics of liver fibrosis assisted by a bedside clinical chemistry analyzer and an automated pretreatment machine.	Clin Chim Acta.	412(19-20)	1767-72	2011
Sugiyama M, Tanaka Y, Wakita T, Nakanishi M, Mizokami M.	Genetic Variation of the IL-28B Promoter Affecting Gene Expression.	PLoS One	6(10)	e26620	2011
Ito K, Kuno A, Ikehara Y, Sugiyama M, Saito H, Aoki Y, Matsui T, Imamura M, Korenaga M, Murata K, Masaki N, Tanaka Y, Hige S, Izumi N, Kurosaki M, Nishiguchi S, Sakamoto M, Kage M, Narimatsu H, Mizokami M.	LecT-Hepa, a glyco-marker derived from multiple lectins, as a predictor of liver fibrosis in chronic hepatitis C patients.	Hepatology	Apr 26		2012
Wang J, Singh US, Rawal RK, Sugiyama M, Yoo J, Jha AK, Scroggin M, Huang Z, Murray MG, Govindarajan R, Tanaka Y, Korba B, Chu CK.	Antiviral activity of novel 2'-fluoro-6'-methylene-carbocyclic adenosine against wild-type and drug-resistant hepatitis B virus mutants.	Bioorg Med Chem Lett.	21(21)	6328-31	2011

雑誌（2/2）

発表者氏名	論文タイトル名	発表誌名	巻号	ページ	出版年
Matsumoto A, Tanaka E, Suzuki Y, Kobayashi M, Tanaka Y, Shinkai N, Hige S, Yatsuhashi H, Nagaoka S, Chayama K, Tsuge M, Yokosuka O, Imazeki F, Nishiguchi S, Saito M, Fujiwara K, Torii N, Hiramatsu N, Karino Y, Kumada H.	Combination of hepatitis B viral antigens and DNA for prediction of relapse after discontinuation of nucleos(t)ide analogs in patient with chronic hepatitis B.	Hepatol Res.	Nov. 22		2011
Tamada Y, Yatsuhashi H, Masaki N, Nakamuta M, Mita E, Komatsu T, Watanabe Y, Muro T, Shimada M, Hijioka T, Satoh T, Mano Y, Komeda T, Takahashi M, Kohno H, Ota H, Hayashi S, Miyakawa Y, Abiru S, Ishibashi H.	Hepatitis B virus strains of sub-genotype A2 with an identical sequence spreading rapidly from the capital region to all over Japan in patients with acute hepatitis B.	Gut.	Nov 7		2011
Fujino T, Nakamuta M, Aoyagi Y, Kohjima M, Satoh T, Fukuda M, Ishibashi H, Yatsuhashi H, Enjoji M.	Early dynamics of viremia in patients with genotype 1b chronic hepatitis C: Peg-IFNalpha2a shows earlier viral decline than peg-IFN alpha2b in combination therapy with ribavirin.	Med Sci Monit.	17(12)		2011
Motomura T, Koga E, Taketomi A, Fukuhara T, Mano Y, Muto J, Konishi H, Toshima T, Uchiyama H, Yoshizumi T, Shirabe K, Maehara Y.	Efficacy of splenectomy in preventing anemia inpatients with recurrenthepatitis C following livertrans-plantation is not dependent on inosine triphosphate pyrophosphatase genotype.	Hepatol Res.	42(3)	288-95	2012

総説

発表者氏名	論文タイトル名	発表誌名	巻号	ページ	出版年
久野 敦、池原 譲、成松 久	カレントテラピー特集「分子腫瘍マーカー：治療標的と経過指標」，グライコプロテオミクスを基軸とした腫瘍マーカー開発技術	ライフメディコム	12/01		2011
Mizokami M.	Discovery of critical host factor, IL-28B, associated with response to HCV treatment.	J Gastro-enterol Hepatol,			2011

Ⅳ. 研究成果の刊行物・別刷

Clinica Chimica Acta 412 (2011) 1767–1772

Contents lists available at ScienceDirect

Clinica Chimica Acta

journal homepage: www.elsevier.com/locate/clinchim

LecT-Hepa: A triplex lectin–antibody sandwich immunoassay for estimating the progression dynamics of liver fibrosis assisted by a bedside clinical chemistry analyzer and an automated pretreatment machine

Atsushi Kuno[a], Yuzuru Ikehara[a], Yasuhito Tanaka[b], Kozue Saito[a], Kiyoaki Ito[c], Chikayuki Tsuruno[d], Shinya Nagai[d], Youichi Takahama[d], Masashi Mizokami[c], Jun Hirabayashi[a], Hisashi Narimatsu[a,*]

[a] Research Center for Medical Glycoscience (RCMG), National Institute of Advanced Industrial Science and Technology (AIST), 1-1-1 Umezono, Tsukuba, Ibaraki 305–8568, Japan
[b] Department of Virology & Liver Unit, Nagoya City University Graduate School of Medical Sciences, Kawasumi, Mizuho, Nagoya 467–8601, Japan
[c] The Research Center for Hepatitis and Immunology, National Center for Global Health and Medicine, Ichikawa, Japan
[d] Product Development Div. 2, Sysmex Corporation, 4-4-4 Takatsukadai, Nishi-ku, Kobe 651–2271, Japan

ARTICLE INFO

Article history:
Received 22 April 2011
Received in revised form 23 May 2011
Accepted 23 May 2011
Available online 30 May 2011

Keywords:
Alpha1-acid glycoprotein
Biomarker
Glycoprotein
Hepatitis C virus
Liver fibrosis
Sandwich immunoassay

ABSTRACT

Background: A quantitative analysis of glyco-alteration in serum glycoproteins provides glyco-parameters for estimating the progression of liver fibrosis. In the analysis of glycans, a manual pretreatment process for clinical specimens leads to a complicated manipulation and loss-of-clinical implementation of the assay.
Method: We evaluated an automated triplex lectin–antibody sandwich immunoassay assisted by an automated protein purification system (ED-01) and a bedside clinical chemistry analyzer (HISCL) for the acquisition of two glyco-parameters (AOL/DSA and MAL/DSA) derived from a fibrosis-related glyco-alteration of serum alpha1-acid glycoprotein (AGP).
Results: We adjusted the auto-machines with their accuracy set to CV <5.0% (ED-01) and <1.0% (HISCL). AGP samples were enriched from 275 serum specimens. Two glyco-parameters obtained by HISCL showed a linear correlation with that from a reported assay (R>0.90). The formula for monitoring fibrosis (LecT-Hepa) was given by a combination of the glyco-parameters. This correlated with the fibrosis stage from biopsy (R = 0.68) and diagnosed severe fibrosis and cirrhosis. It was superior to that of FIB-4 index.
Conclusions: We automated a multilectin-assisted immunoassay with an order of magnitude reduction of operation time without any loss-of-accuracy. LecT-Hepa is a reliable method to assess fibrosis-dynamics from moderate fibrosis to cirrhosis.

1. Introduction

Secreted proteins are practically glycosylated in the endoplasmic reticulum and the Golgi apparatus. Since the features of glycosylation depend on the extent of cell differentiation and the state of the cell, i.e., the origin of a tissue, its developmental stage and the presence of malignancy, blood glycoproteins consist of a mixture of heterogeneous molecules derived from many sources [1,2]. Thus, glycoproteins that exhibit disease-associated glyco-alteration and are present in serum have the potential to act as biomarkers for the diagnosis of a target disease. Numerous glycoproteins have been studied to date as candidate glyco-biomarkers accompanied by rapid advances in glycomics technologies. Such glyco-markers have attracted a great deal of attention in the "discovery phase" of clinical applications [3].

Hepatitis B and C viral (HBV, HCV) infections are prevalent health problems, affecting 350 million and 170 million people, respectively, worldwide. This situation is becoming worse because chronic hepatitis (CH) caused by HCV infection will result in an increase in the incidence of liver cirrhosis (LC) accompanied by an irreversible progression of fibrosis. As about 80% of LC patients (the worst fibrosis stage) have contracted hepatocellular carcinoma (HCC) within the past 10 y, >90% of HCC cases in Japan have originated from chronic hepatitis caused by HCV (81%) or HBV (13%) infection. It is evident that the best way of monitoring the progression of hepatitis is to establish an accurate serological method for the quantitative evaluation of fibrosis, as well as the early detection of HCC. Consequently, a large variety of noninvasive methods have been developed [4], including FibroScan [5], which physically analyzes the progression of liver fibrosis based on transient elastography, and FibroTest [6,7] and Hepascore [8], which are serological tests employing a narrow and complex algorithm derived using a patient's age, sex and biochemical markers. Recently, FIB-4, which uses the patient's age, aspartate aminotransferase (AST), alanine aminotransferase (ALT) and platelet count, has been developed as a simple, inexpensive and accurate fibrosis index in patients with HCV [9–11].

Detecting hepatic disease-associated glyco-markers for clinical applications has been a continuous challenge since the early 1990s,

* Corresponding author. Tel.: +81 29 861 3200.
E-mail address: h.narimatsu@aist.go.jp (H. Narimatsu).

0009-8981/$ – see front matter © 2011 Elsevier B.V. All rights reserved.
doi:10.1016/j.cca.2011.05.028

because increased fucosylation on complex-type *N*-glycans has been frequently detected in glycoproteins from patients with HCC and LC [12–14]. Of all the alpha-fetoprotein (AFP) glycoforms, more than 30% have been found to react to a fucose-binding lectin, *Lens culinaris* agglutinin. This fraction, designated as AFP-L3, was approved by the US FDA in 2005 for the diagnosis and prognosis of HCC [13]. Recently, an immunoassay system for AFP-L3 was automated by combining affinity electrophoresis and recent microfluidics technology [15]. Other challenges have been proposed for diagnosing liver cirrhosis and HCC using recent technology for glycan analysis [16–20]. Callewaert et al. have developed a series of glycan-based liver disease tests [16,17,21,22] based on a capillary electrophoresis-based DNA sequencer. They found that the ratio between two disease-specific glycans helps in the accurate monitoring of liver fibrosis and the diagnosis of compensated cirrhosis and HCC in cirrhosis patients [21]. This system has a big advantage in terms of simplicity over other highly reliable serological tests, such as FibroTest, which measure the α2-macroglobulin/apolipoprotein A-I ratio using two different analyzers. This system had been developed further in terms of a higher throughput and rapid glycan profiling using microfluidics for its clinical implementation [22]. However, this system requires a three-hour manual pretreatment process, i.e., protein denaturation, release of *N*-glycans, desialylation and labeling.

In the context of the development of a fibrosis-related glycoprotein marker, an acute-phase protein alpha1-acid glycoprotein (AGP) is thought to be one of the best candidates, because it is a well-characterized glycoprotein with five highly branched complex-type *N*-glycans, whose alteration (e.g., fucosylation and desialylation) occurs during the progression of liver fibrosis and carcinogenesis [12]. Using these properties, an increased degree of fucosylation was detected in cirrhosis patients using a fucose-binding lectin (AAL)-antibody sandwich ELISA employing an automated analyzer [23]. The detection of asialo-AGP using lactosamine-recognition lectin RCA120 has been reported as an alternative method for detecting cirrhosis, and a rapid immunochromatographic strip test has been developed [24–26]. Recently, we further optimized this useful lectin set for monitoring fibrosis using an antibody-assisted lectin profiling system (ALP) [27]. A multiplex sandwich immunoassay using a 43-lectin microarray detected many other aspects of glyco-alteration of AGP, resulting in the selection of two lectins (*Maackia amurensis* lectin (MAL) and *Aspergillus oryzae* lectin (AOL)) and *Datura stramonium* lectin (DSA) as a fibrosis indicator and a signal normalizer [28]. The resulting two glyco-parameters (AOL/DSA and MAL/DSA) gave a definitive criterion formula that distinguished well between LC and CH patients with a diagnostic accuracy of >90%. We confirmed that the use of this lectin set was statistically superior to previously selected lectins, including AAL and RCA120. This triplex-sandwich immunoassay employing DSA/MAL/AOL lectins and an anti-AGP antibody is expected to be further simplified to be able to be performed by bedside clinical chemistry analyzers. In this study, we evaluated the clinical implementation of our triplex assay. We adopted an automated protein purification machine, the Enrichment Device (ED-01; GP BioSciences Ltd., Yokohama, Japan) (shown in the schematic diagram in Fig. 1) to immunoprecipitate AGP from serum in a rapid, high-throughput and reproducible manner. To enable simple manipulation and a high diffusion rate of the assay, we shifted the detection system from the lectin microarray to a fully automated immunoassay analyzer (HISCL-2000i). The resulting criterion formula for detecting liver fibrosis (LecT-Hepa) was compared with the following fibrosis markers and indices: FIB-4 [9–11], hyaluronic acid (HA) [29,30] and Type IV collagen (IV-Col) [31].

2. Materials and methods

2.1. Patient samples, biochemical parameters and indices

The 175 patients with chronic hepatitis C used as the case subjects were identical to those used in our previous report [28]. The control

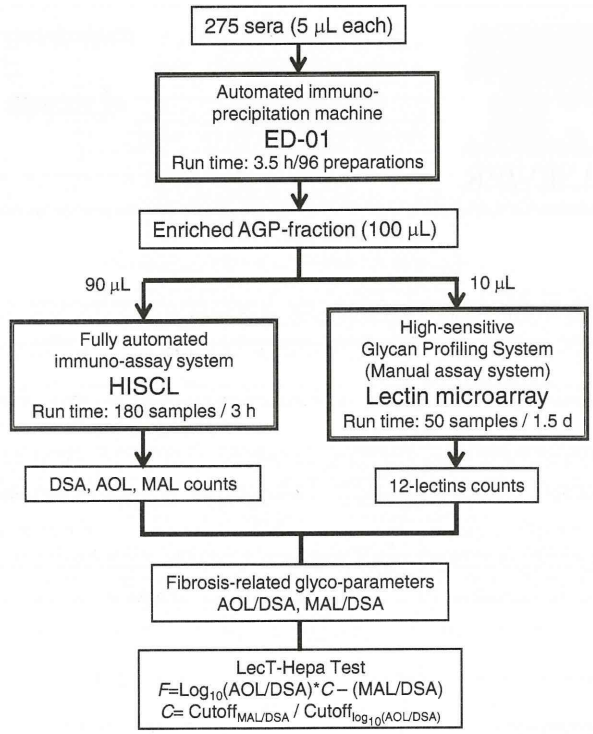

Fig. 1. Schematic diagram for evaluating the progression dynamics of liver fibrosis.

subjects were population-based samples from 100 randomly selected healthy volunteers aged 22–77 y. All sera were collected at Nagoya City University Hospital. The institutional ethics committees at Nagoya City University Hospital and National Institute of Advanced Industrial Science and Technology (AIST) approved this study, and informed consent for the use of their clinical specimens was obtained from all individuals before collection at Nagoya City University Hospital and AIST. Fibrosis was graded for 125 patients according to the Histologic Activity Index using biopsy or surgical specimens. For all patients, the following biological parameters were determined at the time of blood collection: aspartate aminotransferase (AST), alanine aminotransferase (ALT) and platelet count. Serum HA and IV-Col were measured using Latex Agglutination Turbidimetric Immunoassay (SRL Inc, Tokyo, Japan). The FIB-4 index was calculated as follows: [age (years) × AST (U/l)]/[platelets (10^9/l) × ALT (U/l)$^{1/2}$] [9].

2.2. Immunoprecipitation of AGP from serum using an automated protein purification system

We employed an automated protein purification system (ED-01; GP BioSciences Ltd.) to immunoprecipitate AGP from a serum. The working reagents and protocol were followed as listed in a previous report [28], but were optimized for the machine. In brief, all the sera were diluted in a ratio of 1:10 with PBS containing 0.2% SDS, and then heated at 95 °C for 20 min. The resulting solution (50 μl) was mixed with 10 μl of Triton X-100 in TBS (TBSTx) and injected into a 96-well SUMILON microtiter plate (Sumitomo Bakelite Co. Ltd., Tokyo, Japan). The plate and working reagents, which included the biotinylated anti-AGP antibody (50 ng/μl), the streptavidin-immobilized magnetic bead, the washing buffer (1% TBSTx) and the elution buffer (TBS containing 0.2% SDS), were set into the designated position in the machine. After setting the materials, the AGPs (110 μl) were automatically purified (96 samples for 3.5 h).

2.3. A rapid lectin–antibody sandwich immunoassay using HISCL

Fibrosis-specific glyco-alteration of AGP was qualified from simultaneous measurements of the lectin–antibody sandwich immunoassays using three lectins (DSA, MAL and AOL). In principle, the glycan part of the AGP was captured by the lectin immobilized on the magnetic beads, and the captured AGP was then quantified by an anti-human AGP mouse monoclonal antibody probe that was cross-linked to an alkaline phosphatase (ALP-αAGP). The assay manipulation was fully automated using a chemiluminescence enzyme immunoassay machine (HISCL-2000i; Sysmex Co., Kobe, Japan). Four reagent packs, i.e., an AGP-DSA detection reagent pack, an AGP-MAL detection reagent pack, an AGP-AOL detection reagent pack and a chemiluminescence substrate reagent pack, were placed into position in the HISCL machine. Each detection reagent pack comprised three reagents: a reaction buffer solution (R1), a lectin-coated magnetic beads solution (R2) and an ALP-αAGP solution (R3). The chemiluminescence substrate reagent pack contained a CDP-Star substrate solution (R4) and a stopping solution (R5). A representative procedure for the DSA-antibody sandwich assay is described as follows. An aliquot of the AGP-enriched solution (30 μl) was diluted to 60 μl with the R1 solution, and then mixed with the R2 solution (30 μl). After the binding reaction, the R3 reagent (100 μl) was added to the reaction solution. The resulting conjugates were magnetically separated from any unbound AGPs and ALP-αAGP, and substantially mixed with R4 (50 μl) and R5 (100 μl). The chemiluminescent intensity was acquired over a period of 17 min in the operation described above. The reaction chamber was kept at a temperature of 42 °C during the HISCL measurements. The MAL-AGP and AOL-AGP sandwich assays were performed using the same procedure.

2.4. Glycan profiling of AGP using a lectin microarray

The enriched AGPs were subjected to an antibody-overlay lectin microarray [27,28,32] to validate the glycan profiles of the serum AGPs. An aliquot of the purified proteins (4 μl) was diluted to 60 μl with PBS containing 1% Triton X-100 (PBSTx); this was then applied to a LecChip™ (GP BioSciences Ltd.), which included three spots of 45 lectins in each of seven reaction wells. After incubation for 12 h, an excess blocker glycoprotein (2 μl of nonlabeled human serum IgG (10 mg/ml)) was added to the chip and incubated for 30 min. The reaction solution was then discarded, and the chip was washed 3 times with PBSTx. A volume of 60 μl of 50 ng of a biotinylated antibody solution in PBSTx was then applied to the chip, and incubated for 1 h. After three washes with PBSTx, 60 μl of 100 ng of a Cy3-labeled streptavidin (GE Healthcare Buckinghamshire, UK) solution in PBSTx was added and incubated for 30 min. The chip was rinsed with PBSTx and scanned using an evanescent-field fluorescence scanner (GlycoStation™ Reader1200; GP BioSciences Ltd.). We analyzed all the data using the Array Pro Analyzer software package, version 4.5 (Media Cybernetics, Inc., Bethesda, MD). The net intensity value for each spot was calculated by subtracting the background value from the signal intensity values of the 3 spots. We elected to scan data under appropriate gain conditions, which provided the intensities of all positive spots as <40,000. The relative intensities of the positive lectins were determined from their ratio to the fluorescent intensity of the internal-standard lectin DSA.

2.5. Statistics

We performed statistical analyses using the Dr. SPSS II software package for Windows (SPSS Co., Tokyo, Japan), Origin version 8.0 software package for Windows (LightStone Co., Tokyo, Japan) and Excel 2007 for Windows to compare the diagnostic value of the LecT-Hepa test with other serological fibrosis markers or indices. The correlation of the biomarkers with liver fibrosis was estimated from the samples obtained from 110 patients from the correlation coefficient (R) and the *P*-values were calculated using a nonparametric test (the Mann–Whitney *U*-test). To assess the classification efficiencies of various markers for detecting significant fibrosis, severe fibrosis and cirrhosis [33], the receiver operating characteristic (ROC) curve analysis was also carried out to determine the area under the curve (AUC) values. We used the cutoff values obtained from Youden's index [34] to classify the patients. The diagnostic accuracy was expressed as the diagnostic specificity, sensitivity, positive predictive value (PPV), negative predictive value (NPV), overall accuracy and AUC [35].

3. Results and discussion

3.1. Optimization of an automated protein purification machine for AGP enrichment

We first optimized an automated protein purification machine (ED-01) from GP BioSciences to enrich the serum AGP, which was subjected to a rapid and automated triplex lectin–antibody sandwich immunoassay using HISCL to acquire the fibrosis-related glyco-parameters (Fig. 1). To achieve this, we considered the significant difference in the reaction conditions between the automatic assay and a previous manual assay using a lectin microarray. In brief, in the case of HISCL, the binding reaction between the lectin-coated magnetic beads and the analyte AGP must occur within a period of <5 min. In the case of the lectin microarray, the analyte was incubated with lectins immobilized on a glass slide for >12 h. For these reasons, the AGP was enriched from 5 μl of serum for HISCL, which was an order of magnitude larger than that of the lectin microarray (0.5 μl of serum used). The amount of the capturing biotinylated antibody for HISCL was additionally increased to 1 μg per sample, which was five times larger than that of the lectin microarray. These modifications resulted in us obtaining a sufficient amount of AGPs to complete a triplex sandwich assay using HISCL (data not shown). Next, we examined the accuracy of the auto-machine. Sera from a normal healthy volunteer and a patient with HCC were randomly divided into 44 and 3 wells on a 96-well microtiter plate, respectively. PBSTx as a blank was added into a well at the same time. The dispensed plate was then subjected to automatic immunoprecipitation. After a 3.5 h automatic immunoprecipitation period, each enriched AGP was quantitatively compared using the signal intensity of the DSA lectin acquired by the antibody-overlay lectin microarray analysis, which was used as an internal standard because the intensity correlated well with the amount of AGP [28]. From the result from the normal healthy volunteer, the intensity of DSA was averaged to 30,304 with high reproducibility (SD = 1506, CV = 4.97%) (Supplementary Table 1). The quality of the enriched AGP was maintained at a high level to distinguish the glycosylation alteration of AGPs accompanied by the progression of liver fibrosis, i.e., distinction of glycan profiles between the normal healthy volunteer and the patient with HCC using lectin microarray, as reported previously (Supplementary Fig. 1 and Ref. [28]). Collectively, automation of the pretreatment process was optimized to provide the enriched AGP for the next automated sandwich assay (Fig. 1).

3.2. Measurement of a triplex lectin–antibody immunoassay using HISCL

HISCL is an automated sandwich immunoassay system based on the luminescence-assisted detection principle employing a capturing antibody immobilized on magnetic beads and a detection antibody conjugated with alkaline phosphatase. As the HISCL measurement completes within 17 min for clinical implementation, each antigen–antibody interaction reaction must be rapid and strong enough to detect the antigen within the operation time. On the other hand, the glycan (glycoprotein)–lectin interaction is significantly weaker than the antigen–antibody interaction. To overcome this problem in terms of its clinical usefulness, we adapted "high density" lectin magnetic beads. Because our target glycoprotein AGP bore five highly branched

N-glycans, an obviously strong cluster effect was expected to occur from the interaction between the immobilized lectin and the glycans of AGP. In addition, a high abundance of AGP in the sera (0.5–1.0 mg/ml) made it possible to undergo an immediate reaction on the immobilized lectin from the high concentration of the analyte AGP. Keeping in mind these considerations, we evaluated a triplex lectin–antibody immunoassay for the serum AGP using HISCL. The AGPs were enriched from pooled human sera for quality control (Nissui Pharmaceutical Co., Tokyo, Japan) and pooled plasma for the HCV patients. The former was used to measure the lectin–antibody sandwich assays with MAL and DSA, and the latter was used for the assay with AOL. The simultaneous repeatability of each assay was evaluated by performing 10 independent experiments. The resulting coefficient of variation (CV) was in the range 0.6%–1.0%. The sensitivity was evaluated by performing the assay on a serial dilution of the enriched AGP solution from a dilution ratio in the range $1/2^5$ to $1/2^0$ to generate a standard curve. As a negative control, the assay was carried out in the absence of AGP. The background luminescence value (9277 for DSA, 3839 for MAL and 93078 for AOL) was subtracted from the values obtained from all the samples. A linear regression revealed the linear range of detection (R^2>0.99), at least within the above dilution ratio (Fig. 2a–c). The linear range was sufficient to quantify the glyco-alteration of AGP, since the quantification of the glyco-alteration in the previous lectin microarray analysis was performed using AGP concentrations within the range of the five serial dilutions. Taken together, the rapid and automated system performed a triplex lectin–antibody sandwich immunoassay for detecting glyco-alteration of AGP with high reliability.

3.3. *Similarities of the 2 glyco-parameters obtained using HISCL to those obtained using lectin microarray*

Next, we examined whether the 2 fibrosis-related glyco-parameters (AOL/DSA and MAL/DSA) established using the lectin microarray were represented by the HISCL measurements (see schematic diagram in Fig. 1). All the sera used in this study were pretreated in the auto-machine ED-01, as described above, and each enrichment fraction (100 μl) was then divided into a 90 μl portion for HISCL and a 10 μl portion for the lectin microarray. We performed a triplex lectin–antibody sandwich assay using both systems with sera from 275 specimens (175 HCV patients and 100 healthy volunteers), and we then determined the two glyco-parameters. As shown in the resulting scatter plots, the upper limit of detection for HISCL was higher than that of the lectin microarray (Fig. 2d and e). According to the best linear curve with its correlation coefficient and the coefficient of determination (R^2 = 0.91 for AOL/DSA and 0.82 for MAL/DSA), we confirmed that the use of the rapid and automated assay system could acquire the two glyco-parameters.

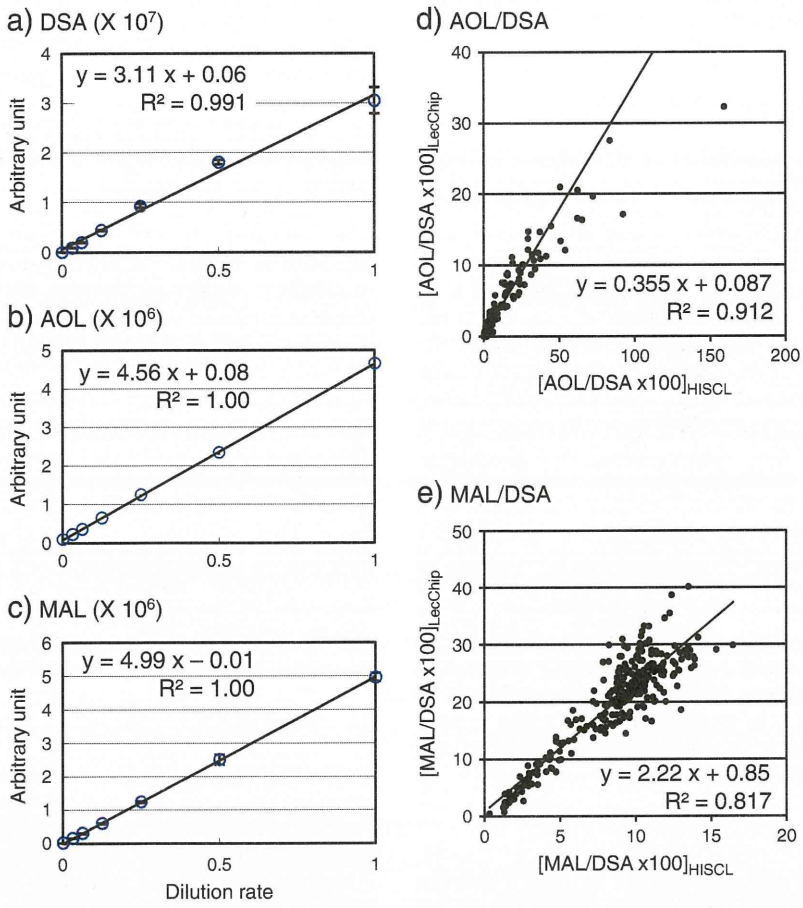

Fig. 2. Rapid operation for obtaining two glyco-parameters (AOL/DSA, MAL/DSA). Standard curves for the quantification of AGPs specifically binding to: (a) DSA, (b) AOL and (c) MAL lectins using an automated lectin–antibody sandwich immunoassay employing HISCL. Each data point represents the mean of triplicate independent experiments with the error bars showing the mean ± standard deviation. Each glyco-parameter (d) AOL/DSA and (e) MAL/DSA was determined using 275 different serum samples for both HISCL and a manual assay employing a lectin microarray. The graphs show scatter plots, and the best linear curve with its correlation coefficient was calculated using the Excel 2007 software package (Microsoft). The plots were limited (<50 for HISCL) in the calculation of the correlation coefficient for AOL/DSA.

3.4. Definition of a criterion formula for estimating the progression of liver fibrosis

To assess the correlation of the two obtained glyco-parameters with the progression of fibrosis, we analyzed the data from HISCL measurements on 125 HCV patients (F0–F1, 26.4% (33 patients); F2, 25.6% (32 patients); F3, 24% (30 patients); and F4, 23.2% (29 patients)). As shown on the left-hand side of Supplementary Fig. 2, the MAL/DSA values gradually decreased with the progression of fibrosis, and the Pearson's correlation coefficient was R = −0.67. On the other hand, the AOL/DSA values increased exponentially. Indeed, the Pearson's correlation coefficient of Log_{10}(AOL/DSA) was R = 0.68, which is higher than that of AOL/DSA (R = 0.51). Both parameters fitted for the quantification of the progression of fibrosis from F2 to F4. Next, we examined the AUC to characterize the diagnostic accuracy of cirrhosis (F4). For the prediction of cirrhosis, the AUC, diagnostic sensitivity, diagnostic specificity and the cutoff value of AOL/DSA were 0.89 (95% CI 0.82–0.97), 89%, 81% and 4.15, respectively (right-hand side of Supplementary Fig. 2). MAL/DSA could detect cirrhosis with an AUC = 0.85 (95% CI 0.83–0.97), a diagnostic sensitivity of 85%, a diagnostic specificity of 88% and a cutoff value of 5.31. These values suggest that AOL/DSA tended to favor sensitive detection, whereas the MAL/DSA functions suppressed the pseudo positive rate. We developed the following criterion formula, named the "LecT-Hepa Test", to enhance the diagnostic accuracy by combining both glyco-parameters:

$$F = \mathrm{Log}_{10}[\mathrm{AOL}/\mathrm{DSA}]^{*}C - [\mathrm{MAL}/\mathrm{DSA}], \text{ and}$$

$$C = \mathrm{Cutoff}_{\mathrm{MAL}/\mathrm{DSA}} / \mathrm{Cutoff}_{\mathrm{log10(AOL}/\mathrm{DSA)}}$$

where Cutoff_x is the cutoff value for distinguishing liver cirrhosis in the 125 patients by glyco-parameter X. In this study, we calculated a value of $C = 5.31/\mathrm{Log}_{10}4.15 = 8.6$. The LecT-Hepa Test correlated well with the progression of fibrosis (R = 0.68). In addition, we tested the accuracy of LecT-Hepa for the diagnosis of liver cirrhosis using a validation data set from another 88 patients (liver cirrhosis, $n = 45$; chronic hepatitis, $n = 43$) used in a previous report [28]. The LecT-Hepa detected liver cirrhosis with a diagnostic sensitivity of 91% and a diagnostic specificity of 91%, whereas AOL/DSA and MAL/DSA had a diagnostic sensitivity of 91% and a diagnostic specificity of 89%, and a diagnostic sensitivity of 77% and a diagnostic specificity of 96%, respectively. Furthermore, the pseudo positive rates of MAL/DSA, AOL/DSA and LecT-Hepa targeted from 100 normal healthy volunteers were 0%, 11% and 2%, respectively. These results indicate that the use of the rapid and automated assay system to acquire a fibrosis-related formula (LecT-Hepa) comprising the two glyco-parameters was valid.

3.5. Comparison of serological fibrosis biomarkers and indices

Finally, we compared the diagnostic accuracy of each lectin value at each stage of fibrosis, i.e., significant fibrosis (F2, F3 and F4), severe fibrosis (F3 and F4) and cirrhosis (F4), between LecT-Hepa and other fibrosis markers. HA and IV-Col were selected as comparable fibrosis markers acquired by the single biomarker measurement, as well as FIB-4, which is well known as an inexpensive and accurate fibrosis index of four parameters obtained in general blood tests [9–11]. In this examination, the objective specimens were limited to the sera from 110 patients (F0, 1 = 32, F2 = 32, F3 = 28 and F4 = 18) because of their availability for all parameters, i.e., age, platelet count, AST, ALT, HA, IV-Col, AOL/DSA and MAL/DSA. The resulting serum levels and the distribution of fibrosis markers and indices are shown in Supplementary Table 2 and Fig. 3. On comparing the correlation coefficient between these data, we found that LecT-Hepa (R = 0.68) was the best for estimating fibrosis dynamics. Although all the tests including LecT-Hepa increased exponentially with the progression of fibrosis, LecT-Hepa particularly distinguished between F2, F3 and F4 patients. The observation

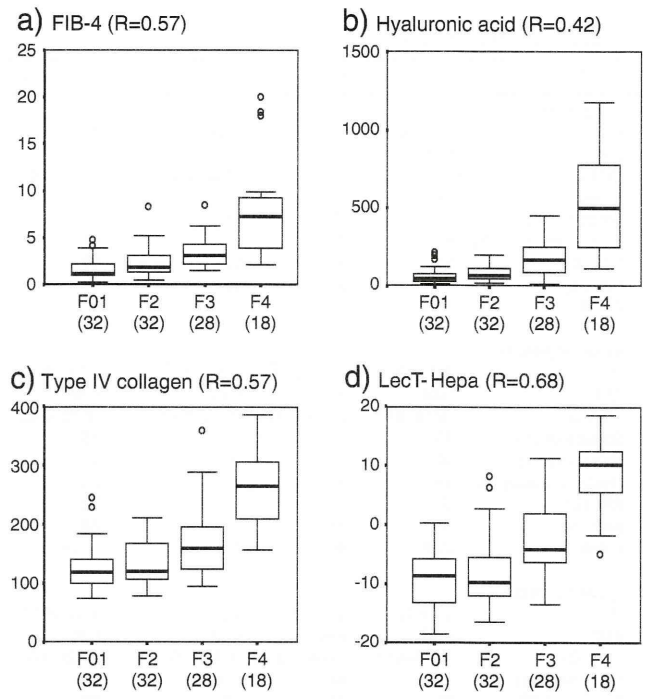

Fig. 3. Correlation of four fibrosis markers with the progression of liver fibrosis. Box–whisker plots according to the Histologic Activity Index show the 75th and 25th percentiles (the top and bottom of the box, respectively), the median (line through the middle of the box) and the 95th and 5th percentiles (the top and bottom of the whiskers, respectively), as well as the R, Pearson's correlation coefficient between the fibrosis stage from biopsy and the fibrosis markers.

was supported by the following estimation using a nonparametric test (the Mann–Whitney *U*-test) and ROC investigation (Table 1). Because the ROC curves were compiled to estimate their cutoff values using the data set from 110 patients (F0, 1, 2, 3 = 92, F4 = 18), the number of patients with fibrosis stage F4 was not sufficient to compare the diagnostic values for detecting cirrhosis. For this reason, we used an additional 19 patients with LC determined using ultrasonography (coarse liver architecture, nodular liver surface and blunt liver edges) and evidence of hypersplenism (splenomegaly in the ultrasonography) in 175 HCV patients. As a result, LecT-Hepa could still detect liver cirrhosis with high diagnostic accuracy (diagnostic sensitivity of 89%, diagnostic specificity of 86%, overall accuracy of 87%, PPV of 72% and NPV of 95%), which is superior to the values of FIB-4 (diagnostic sensitivity of 84%, diagnostic specificity of 83%, overall accuracy of 83%, PPV of 66% and NPV of 93%) and HA (diagnostic sensitivity of 95%, diagnostic specificity of 74%, overall accuracy of 80%, PPV of 59% and NPV of 97%). Interestingly, the false diagnosis cases with LecT-Hepa were not necessarily identical to those with FIB-4 (Supplementary Table 3). This suggests that a combination of LecT-Hepa and FIB-4 would be effective.

4. Conclusions

We developed a triplex lectin–antibody immunoassay using a bedside clinical chemistry analyzer. This allows a marked reduction in operation time from 12 h to <30 min per triplex assay of a sample, resulting in its clinical usefulness. The reliability was secured by the full automation of the pretreatment process. The diagnostic score of LecT-Hepa was superior to that of other serological indices and markers. Consequently, LecT-Hepa evolved reliably to assess the dynamics of fibrosis from moderate fibrosis to cirrhosis. Further validation tests are underway.

Supplementary materials related to this article can be found online at doi:10.1016/j.cca.2011.05.028.

Table 1
Diagnostic values of the fibrosis markers.

$n=110$	FIB-4	HA	Type IV collagen	LecT-Hepa
a) Significant fibrosis				
P^a	2.5×10^{-6}	4.2×10^{-6}	1.2×10^{-4}	7.5×10^{-5}
AUC	0.78	0.77	0.73	0.73
(95% CI)	(0.68–0.87)	(0.67–0.87)	(0.62–0.84)	(0.63–0.85)
Sensitivity (%)	92	68	59	63
Specificity (%)	53	78	88	78
Overall accuracy (%)	81	71	67	67
PPV (%)	83	88	92	88
NPV (%)	74	50	47	46
Cutoff	1.23	85	151	−5.8
b) Severe fibrosis				
P^a	1.7×10^{-10}	6.3×10^{-12}	4.0×10^{-9}	1.3×10^{-11}
AUC	0.84	0.86	0.82	0.86
(95% CI)	(0.76–0.91)	(0.79–0.93)	(0.74–0.89)	(0.79–0.92)
Sensitivity (%)	83	85	78	85
Specificity (%)	70	77	80	77
Overall accuracy (%)	76	80	79	80
PPV (%)	67	72	74	72
NPV (%)	85	88	84	88
Cutoff	2.29	90	152	−5.6
c) Liver cirrhosis				
P^a	2.7×10^{-8}	2.2×10^{-10}	1.2×10^{-10}	1.4×10^{-12}
AUC	0.88	0.92	0.92	0.95
(95% CI)	(0.80–0.96)	(0.84–1.0)	(0.85–1.0)	(0.89–1.0)
Sensitivity (%)	78	94	100	94
Specificity (%)	83	74	70	86
Overall accuracy (%)	82	77	75	87
PPV (%)	47	42	39	57
NPV (%)	95	99	100	99
Cutoff	3.88	141	156	−1.8

[a] *P* value calculated using a nonparametric test (the Mann–Whitney *U*-test).
AUC = area under the receiver operating characteristic curve; PPV = positive predictive value; NPV = negative predictive value.

Abbreviations

AGP	alpha1-acid glycoprotein
AOL	*Aspergillus oryzae* lectin
AP	alkaline phosphatase
CH	chronic hepatitis
DSA	*Datura stramonium* agglutinin
HA	hyaluronic acid
LC	liver cirrhosis
MAL	*Maackia amurensis* lectin
PBSTx	phosphate-buffered saline containing 1% Triton X-100
TBSTx	tris-buffered saline containing 1% Triton X-100
IV-Col	Type IV collagen

Acknowledgements

This work was supported in part by a grant from New Energy and Industrial Technology Development Organization of Japan. We are very grateful to S. Unno, H. Shimazaki, T. Fukuda (AIST), Y. Hamaguchi, T. Kagawa, S. Matsubara, M. Terao (Sysmex Co.), A. Saito and K. Yokota (GP BioSciences) for technical assistance or critical suggestion on assay development.

References

[1] Dennis JW, Laferte S, Waghorne C, Breitman ML, Kerbel RS. Beta1-6 branching of Asn-linked oligosaccharides is directly associated with metastasis. Science 1987;236:582–5.
[2] Granovsky M, Fata J, Pawling J, Muller WJ, Khokha R, Dennis JW. Suppression of tumor growth and metastasis in Mgat5-dificient mice. Nat Med 2000;6:306–12.
[3] Taniguchi N, Hancock W, Lubman DM. Rudd PM The second golden age of glycomics: from functional glycomics to clinical applications. J Proteome Res 2009;8:425–6.
[4] Jarcuska P, Janicko M, Veselíny E, Jarcuska P, Skladaný L. Circulating markers of liver fibrosis progression. Clin Chim Acta 2010;411:1009–17.
[5] Castéra L, Vergniol J, Foucher J, et al. Prospective comparison of transient elastography, Fibrotest, APRI, and liver biopsy for the assessment of fibrosis in chronic hepatitis C. Gastroenterology 2005;128:343–50.
[6] Imbert-Bismut F, Ratziu V, Pieroni L, et al. Biochemical markers of liver fibrosis in patients with hepatitis C virus infection: a prospective study. Lancet 2001;357: 1069–75.
[7] Gressner OA, Beer N, Jodlowski A, Gressner AM. Impact of quality control accepted inter-laboratory variations on calculated Fibrotest/Actitest scores for the non-invasive biochemical assessment of liver fibrosis. Clin Chim Acta 2009;409:90–5.
[8] Guéchot J, Lasnier E, Sturm N, Paris A, Zarski JP. ANRS HC EP 23 Fibrostar study group. Automation of the Hepascore and validation as a biochemical index of liver fibrosis in patients with chronic hepatitis C from the ANRS HC EP 23 Fibrostar cohort. Clin Chim Acta 2010;411:86–91.
[9] Sterling RK, Lissen E, Clumeck N, et al. Development of a simple noninvasive index to predict significant fibrosis in patients with HIV/HCV coinfection. Hepatology 2006;43:1317–25.
[10] Vallet-Pichard A, Mallet V, Nalpas B, et al. FIB-4: an inexpensive and accurate marker of fibrosis in HCV infection. Comparison with liver biopsy and fibrotest. Hepatology 2007;46:32–6.
[11] Trang T, Petersen JR, Snyder N. Non-invasive markers of hepatic fibrosis in patients co-infected with HCV and HIV: comparison of the APRI and FIB-4 index. Clin Chim Acta 2008;397:51–4.
[12] Turner GA. N-glycosylation of serum proteins in disease and its investigation using lectins. Clin Chim Acta 1992;208:149–71.
[13] Sato Y, Nakata K, Kato Y, et al. Early recognition of hepatocellular-carcinoma based on altered profiles of alpha-fetoprotein. N Eng J Med 1993;328:1802–6.
[14] Ohkura T, Hada T, Higashino K, et al. Increase of fucosylated serum cholinesterase in relation to high risk groups for hepatocellular carcinomas. Cancer Res 1994;54:55–61.
[15] Kagebayashi C, Yamaguchi I, Akinaga A, et al. Automated immunoassay system for AFP-L3% using on-chip electrokinetic reaction and separation by affinity electrophoresis. Anal Biochem 2009;388:306–11.
[16] Callewaert N, Van Vlierberghe H, Van Hecke A, et al. Noninvasive diagnosis of liver cirrhosis using DNA sequencer-based total serum protein glycomics. Nat Med 2004;10:429–34.
[17] Liu X-E, Desmyter L, Gao CF, et al. N-glycomic changes in hepatocellular carcinoma patients with liver cirrhosis induced by hepatitis B virus. Hepatology 2007;46: 1426–35.
[18] Mehta AS, Long RE, Comunale MA, et al. Increased levels of galactose-deficient anti-Gal immunoglobulin G in the sera of hepatitis C virus-infected individuals with fibrosis and cirrhosis. J Virol 2008;82:1259–70.
[19] Comunale MA, Wang M, Hafner J, et al. Identification and development of fucosylated glycoproteins as biomarkers of primary hepatocellular carcinoma. J Proteome Res 2009;8:595–602.
[20] Debruyne EN, Vanderschaeghe D, Van Vlierberghe H, Vanhecke A, Callewaert N, Delanghe JR. Diagnostic value of the hemopexin N-glycan profile in hepatocellular carcinoma patients. Clin Chem 2010;56:823–31.
[21] Vanderschaeghe D, Laroy W, Sablon E, et al. GlycoFibroTest is a highly performant liver fibrosis biomarker derived from DNA sequencer-based serum protein glycomics. Mol Cell Proteomics 2009;8:986–94.
[22] Vanderschaeghe D, Szekrényes A, Wenz C, et al. High-throughput profiling of the serum N-glycome on capillary electrophoresis microfluidics systems: toward clinical implementation of GlycoHepatoTest. Anal Chem 2010;82:7408–15.
[23] Rydén I, Påhlsson P, Lindgren S. Diagnostic accuracy of alpha(1)-acid glycoprotein fucosylation for liver cirrhosis in patients undergoing hepatic biopsy. Clin Chem 2002;48:2195–201.
[24] Song EY, Kim KA, Kim YD, et al. Elevation of serum asialo-alpha(1) acid glycoprotein concentration in patients with hepatic cirrhosis and hepatocellular carcinoma as measured by antibody–lectin sandwich assay. Hepatol Res 2003;26:311–7.
[25] Lee EY, Kang JH, Kim KA, et al. Development of a rapid, immunochromatographic strip test for serum asialo alpha1-acid glycoprotein in patients with hepatic disease. J Immunol Methods 2006;308:116–23.
[26] Kim KA, Lee EY, Kang JH, et al. Diagnostic accuracy of serum asialo-alpha1-acid glycoprotein concentration for the differential diagnosis of liver cirrhosis and hepatocellular carcinoma. Clin Chim Acta 2006;369:46–51.
[27] Kuno A, Kato Y, Matsuda A, et al. Focused differential glycan analysis with the platform antibody-assisted lectin profiling for glycan-related biomarker verification. Mol Cell Proteomics 2009;8:99–108.
[28] Kuno A, Ikehara Y, Tanaka Y, et al. Multilectin assay for detecting fibrosis-specific glyco-alteration by means of lectin microarray. Clin Chem 2011;57:48–56.
[29] Guéchot J, Serfaty L, Bonnand AM, Chazouillères O, Poupon RE, Poupon R. Prognostic value of serum hyaluronan in patients with compensated HCV cirrhosis. J Hepatol 2000;32:447–52.
[30] Veillon P, Gallois Y, Moal V, et al. Assessment of new hyaluronic acid assays and their impact on FibroMeter scores. Clin Chim Acta 2011;412:347–52.
[31] Hiramatsu N, Hayashi N, Kasahara A, et al. Improvement of liver fibrosis in chronic hepatitis C patients treated with natural interferon alpha. J Hepatol 1995;22:135–42.
[32] Kuno A, Uchiyama N, Koseki-Kuno S, et al. Evanescent-field fluorescence-assisted lectin microarray: a new strategy for glycan profiling. Nat Methods 2005;2:851–6.
[33] Leroy V, Halfon P, Bacq Y, et al. Diagnostic accuracy, reproducibility and robustness of fibrosis blood tests in chronic hepatitis C: a meta-analysis with individual data. Clin Biochem 2008;41:1368–76.
[34] Akobeng AK. Understanding diagnostic tests 3: receiver operating characteristic curves. Acta Paediatr 2007;96:644–7.
[35] Glas AS, Lijmer JG, Prins MH, Bonsel GJ, Bossuyt PM. The diagnostic odds ratio: a single indicator of test performance. J Clin Epidemiol 2003;56:1129–35.

OPEN ACCESS Freely available online

PLoS one

Genetic Variation of the *IL-28B* Promoter Affecting Gene Expression

Masaya Sugiyama[1,2,5], Yasuhito Tanaka[3], Takaji Wakita[4], Makoto Nakanishi[2], Masashi Mizokami[1]*

1 The Research Center for Hepatitis and Immunology, National Center for Global Health and Medicine, Ichikawa, Chiba, Japan, **2** Department of Biochemistry and Cell Biology, Nagoya City University Graduate School of Medical Sciences, Mizuho, Nagoya, Japan, **3** Department of Virology and Liver Unit, Nagoya City University Graduate School of Medical Sciences, Mizuho, Nagoya, Japan, **4** Department of Virology II, National Institute of Infectious Diseases, Shinjuku, Tokyo, Japan, **5** JSPS Research Fellow, Japan Society for the Promotion of Science, Chiyoda, Tokyo, Japan

Abstract

The current standard of care for the treatment of chronic hepatitis C is pegylated interferon-α (PEG-IFNα) and ribavirin (RBV). The treatment achieves a sustained viral clearance in only approximately 50% of patients. Recent whole genome association studies revealed that single nucleotide polymorphisms (SNPs) around *IL-28B* have been associated with response to the standard therapy and could predict treatment responses at approximately 80%. However, it is not clear which SNP is most informative because the genomic region containing significant SNPs shows strong linkage disequilibrium. We focused on SNPs in close proximity to the *IL-28B* gene to evaluate the function of each and identify the SNP affecting the *IL-28B* expression level most. The structures of *IL-28A/B* from 5′ to 3′-UTR were determined by complete cDNA cloning. Both *IL-28A* and *28B* genes consisted of 6 exons, differing from the CCDS data of NCBI. Two intron SNPs and a nonsynonymous SNP did not affect *IL-28B* gene function and expression levels but a SNP located in the proximal promoter region influenced gene expression. A (TA) dinucleotide repeat, rs72258881, located in the promoter region was discovered by our functional studies of the proximal SNPs upstream of *IL-28B*; the transcriptional activity of the promoter increased gradually in a $(TA)_n$ length-dependent manner following IFN-α and lipopolysaccharide stimulation. Healthy Japanese donors exhibited a broad range of (TA) dinucleotide repeat numbers from 10 to 18 and the most prevalent genotype was 12/12 (75%), differing from the database (13/13). However, genetic variation of *IL-28A* corresponding to that of *IL-28B* was not detected in these Japanese donors. These findings suggest that the dinucleotide repeat could be associated with the transcriptional activity of *IL-28B* as well as being a marker to improve the prediction of the response to interferon-based hepatitis C virus treatment.

Citation: Sugiyama M, Tanaka Y, Wakita T, Nakanishi M, Mizokami M (2011) Genetic Variation of the *IL-28B* Promoter Affecting Gene Expression. PLoS ONE 6(10): e26620. doi:10.1371/journal.pone.0026620

Editor: John E. Tavis, Saint Louis University, United States of America

Received June 29, 2011; **Accepted** September 29, 2011; **Published** October 25, 2011

Funding: This work was supported by a Grant-in-Aid from the Ministry of Health Labor and Welfare of Japan and a Grant-in-Aid from the Ministry of Education, Culture, Sports, Science, and Technology of Japan (271000) and The Grant of National Center for Global Health and Medicine (22–302). The funders had no role in study design, data collection and analysis, decision to publish, or preparation of the manuscript.

Competing Interests: The authors have declared that no competing interests exist.

* E-mail: mmizokami@hospk.ncgm.go.jp

Introduction

A novel group of cytokines was discovered simultaneously by two independent groups in 2003 and named interferon lambda (IFN-λ) [1,2] or type III IFN. Type III IFN comprises three members, IFN-λ1, 2, and 3 or *IL-29* and *IL-28A*, and *IL-28B*, respectively. Type III IFN is a member of the class II cytokine family. This family includes type I, II, and III interferons and the IL-10 family (IL-10, IL-19, IL20, IL-22, IL-24, and IL-26). IFN-λ uses a distinct receptor complex consisting of a unique subunit, named IFN-λR1, and the IL-10R2 subunit. Expression of the IFN-λR1 receptor subunit is highly restricted, whereas the type I IFN receptor complex and the IL-10R2 receptor were detected in most cell types [1,2,3,4,5,6]. The IL-10R2 receptor subunit is shared by IL-10, IL-22, IL-24, IL-26, and IFN-λ. This suggests that type III IFNs act in a rather cell-type specific manner to mediate their biological functions. Type III IFNs trigger a type I IFN-like gene expression profile [5,6,7], which has been shown to have antiviral activity *in vitro* and *in vivo* [1,2,5,6,8]. Thus, the two types of IFN seem to have similar biological effects at a cellular level. IFN-α and IL-29/28A treatment reduced the concentration of hepatitis C virus (HCV) plus-strand RNA in an *in vitro* assay [6,9,10,11]. In addition, IL-29 may have therapeutic value against chronic viral hepatitis in human patients [5].

Recently, a genome-wide association study (GWAS) revealed that several highly correlated common single nucleotide polymorphisms (SNPs), in a linkage disequilibrium (LD) block encompassing the *IL-28B* genes on chromosome 19q13, are implicated in the response of chronic hepatitis C (CHC) patients to pegylated IFN-alpha (PEG-IFNα) and ribavirin (RBV) [12,13,14]. The CC genotype of rs12979860 and TT genotype of rs8099917 are associated in CHC patients with a sustained viral response (SVR) of 2.5 or greater rate, which is dependent of ethnicity, compared to the other genotypes. Moreover, the CC genotype of rs12979860 and TT genotype of rs8099917 favor spontaneous clearance of HCV [15].

We have reported the genomic analysis of approximately 15 kb containing the significant SNPs using Haploview software for LD and haplotype structure [14,16]. To analyze the difference in LD pattern between races, we performed LD mapping with these SNPs on JPT (Japanese in Tokyo), CEU (Utah residents with ancestry from Northern and Western Europe) or YRI (Yoruba in

Ibada, Nigeria) populations. These SNPs were in strong LD in JPT and CEU populations, although relatively low LD was predicted in the YRI population [14,16], suggesting that any of the SNPs located in this region could be responsible for treatment response. Because of the strong LD, tests for independence among these variants were not able to reveal which of these SNPs is uniquely responsible for the association with virological response (VR) or non-virological response (NVR). The identification of the primary genetic variant located in the LD block remained critical, although the risk haplotype tended to influence the expression levels or activity of *IL-28B* [13,14]. In this study, we sought to determine the primary SNP affecting IL-28B expression and/or its function by focusing on the proximal regulatory region of *IL-28B*.

IL-28B was discovered as a member of the IFN-λ family by Sheppard et al. and Kotenko et al. [1,2]. They discovered this family, *IL-29*, *IL-28A*, and *IL-28B* and the specific receptor, *IL-28R1*, by applying individual computational techniques to the draft human genome. However, the start codon of IFN-λ differs between the reports, with an additional 12 nucleotides at the N-terminus in all IFN-λs reported by Sheppard et al. (Fig. S1). The sequence similarity between these ORFs is approximately 96.7% and, especially, there is a high degree of identity between *IL-28A* and *IL-28B* cDNA (approximately 98%). Figure 1A shows the locations of *IL-28A/B* gene, the significant SNPs around *IL-28B* related to anti-HCV therapy reported in previous studies [12,13,14], and $(TA)_n$ repeats in the regulatory region of *IL-28A* and *B*. The SNPs information assessed in this study is summarized in Table 1 and the locations of the SNPs are shown in the schematic of the *IL-28B* gene (Fig. 1B). The reference sequences of *IL-28A* or *IL-28B* cDNA, registered in NCBI CCDS, are composed of 6 exons and 5 exons, respectively (Fig. 1B). Because high sequence similarity was observed between *IL-28A* and *IL-28B* from CpG to the region downstream of 3′-UTR (Fig. S2), the genes were almost completely identical around transcription start site (TSS) (>99%). Then, we determined the likely gene structure using a complete cDNA cloning method because a similar transcriptional mechanism was expected for *IL-28A* and *IL-28B*.

Materials and Methods

Genome samples

Genome samples were obtained from 20 healthy volunteers (HV). Peripheral blood mononuclear cells (PBMC) collected from HV were isolated using the BD Vacutainer CPT Method (BD Biosciences). Genomic DNAs were extracted by standard methods. SNPs were selected from the database at GWAS database (https://gwas.lifesciencedb.jp/cgi-bin/gwasdb/gwas_top.cgi). Written informed consent was provided by all participants in the genotyping study following procedures approved by the Ethical Committee at Nagoya City University.

Cell lines

Human hepatocellular carcinoma cell lines, HepG2 and HuH7, human hepatocyte cell lines, HuSE2 (kindly provided by Dr. Hijikata in Kyoto University), and the human cervical cancer cell line, HeLa (obtained from The American Type Culture Collection), were cultured in Dulbecco's modified Eagle's medium supplemented with 10% (v/v) fetal bovine serum, 100 U ml^{-1} penicillin and 100 mg ml^{-1} streptomycin. Human leukemia virus type 1 transformed cell line, MT-2 (a gift from Dr. Ueda in Nagoya City University), Burkitt lymphoma cell line, Raji, and human T cell leukemia cell line, Jurkat (obtained from The American Type Culture Collection), were cultured in RPMI 1640 medium supplemented with 10% (v/v) fetal bovine serum, 100 U ml^{-1} penicillin and 100 mg ml^{-1} streptomycin. All incubations were performed at 37°C in a 5% CO_2 gassed incubator. Recombinant human IFN-λ2 and -3 were purchased from R&D Systems (Abingdon, UK). Natural human IFN-α was

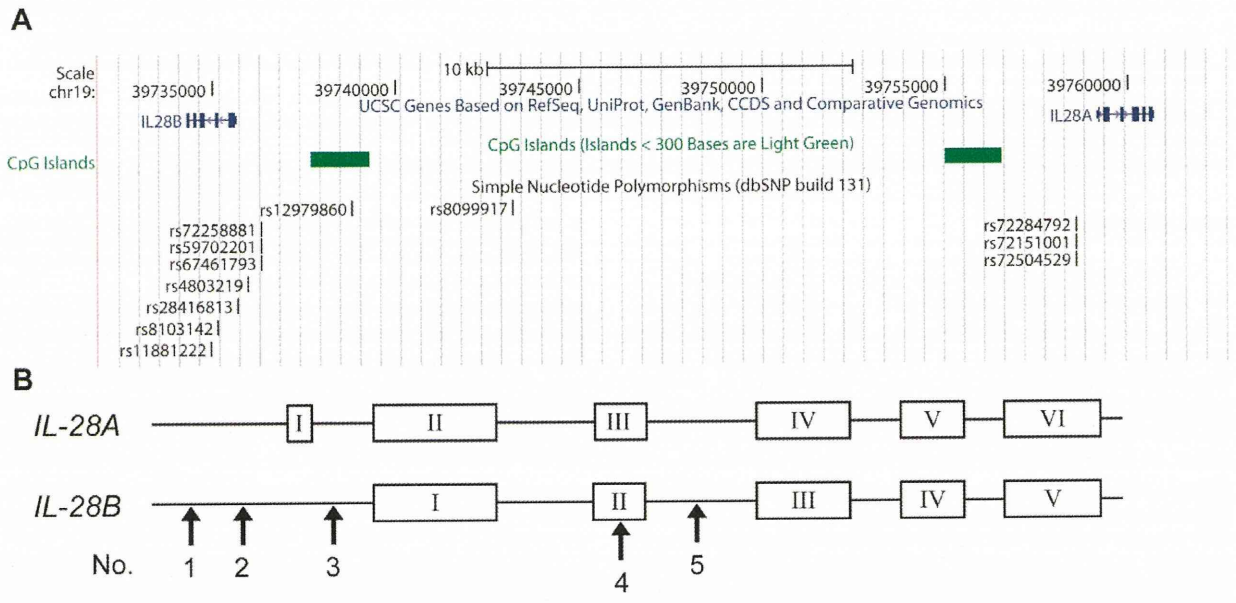

Figure 1. The position of significant SNPs and *IL-28A/B* in chromosome 19, retrieved from the database. (A) The *IL-28A/B* genes located in chromosome 19q13 are described in the genome map of the UCSC genome browser. The significant proximal SNPs around *IL-28B* associated with response to PEG-IFN/RBV therapy are shown in the map [14]. SNPs of $(TA)_n$ variation at the regulatory region of *IL-28A* are displayed in the position corresponding to that of *IL-28B*, which is not associated with anti-HCV therapy. (B) The schematic of *IL-28A/B* gene structure is described based NCBI CCDS data. Arrows show five significant SNPs examined in this study (see Table 1).
doi:10.1371/journal.pone.0026620.g001

Table 1. Significant SNPs around *IL-28B*.

Feature	rs ID	Allele 1/2*[1]	Minus strand*[2]	Location	No.
DIP*[3]	rs72258881*[4]	ATAT/-	TATA/-	Regulatory	1
Substitution	rs4803219	C/T	G/A	Regulatory	2
	rs28416813	C/G	G/C	Intron	3
	rs8103142	T/C	A/G	Nonsynonymous	4
	rs11881222	A/G	T/C	Intron	5

*[1]These data were derived from dbSNP. Allele 2 is the risk allele of HCV therapy reported by Tanaka *et al.*, except for rs72258881.
*[2]Complementary nucleotides are shown because *IL-28B* is coded on the minus strand.
*[3]DIP: deletion/insertion polymorphism.
*[4]The ID represents rs72258881, rs59702201, and rs67461793 because these three are located in the same genomic region, the TA repeat.
doi:10.1371/journal.pone.0026620.t001

purchased from Hayashibara co. ltd. (Okayama, Japan). The mRNA expression levels of receptors stimulated in this study were confirmed by PCR using gene specific primer (Table S1 and Fig. S3),

Plasmid Construction

As a T/G heterozygote genome of rs8099917 with a strong LD was used as the PCR template, amplicons from the major and minor alleles were obtained for the assay described below. PCR was carried out to amplify the fragment from −858 nt of the ATG site to TGA of *IL-28B*, and the products were inserted into pcDNA3.1/Hyg (pcDNA/MA or mi) or pcDNA3.1/Hyg vector deleting CMV promoter (pdCMV/MA or mi). A FLAG sequence was conjugated to 6th exon, removing the stop codon, for real time PCR analysis. The promoter region from nucleotide position −858 to +30 of *IL-28B* was amplified using pdCMV/MA or mi vector and inserted into pGL4 vector for the luciferase assay. A vector with an antisense insert was prepared as a control. For expression constructs, the wild type (WT) plasmids, pcDNA3.1/wild expressing human IL-28B, and pcDNA3.1/ns-mut expressing human IL-28B harboring a $K^{74}R$ mutation, were generated using pcDNA3.1/V5-His-TOPO® (Invitrogen, San Diego, CA) and were used in the subsequent transfections. In addition, pcDNA3.1/AS expressing antisense strand of IL-28B was constructed as a control. We also obtained a pISRE-luc plasmid (provided by Sakamoto N., Tokyo Medical Dental University, Tokyo, Japan). The pGL4.74 vector encoding Renilla Luciferase was purchased from Promega (Madison, WI). These primer sequences are available on request. The above expression vectors were modified for the analysis of splicing function by introducing two intron SNPs (rs28416813 and rs11881222) (Table 1), which were pcDNA/WT, d-iSNPs.

Transient transfections

Transient transfections of HeLa, Jurkat, Raji, HuH7, HepG2, or HuSE2 (hepatocellular carcinomas cell line) cells were carried out using FuGene HD (Roche) or the Cell Line Nucleofector kit (Amaxa Biosystems) according to the manufacturers' protocols. Briefly, Cells (2×10^5) were seeded into a 6 well plate and transfected with for FuGene HD. For the electroporation method, cells (1.0×10^6) were collected and resuspended in Nucleofector solution V for each individual transfection sample.

5′-, 3′-RACE based on full-length cDNA cloning

Total RNA was prepared from cell lines stimulated with lipopolysaccharide (LPS) (0127:B8, Sigma-Aldrich) for 4 hours after 100 U/mL of IFN-α for 16 hours by following previous paper [17]. A GeneRacer Kit (Invitrogen Life Technologies) was used to obtain the complete cDNA sequence of *IL-28A/B* following manufacturer's instructions. Briefly, the GeneRacer RNA Oligo was ligated to the 5′ end specifically of full-length mRNA within the total RNA mixture. This ligated mRNA was then converted to cDNA using reverse transcriptase (RT) and the GeneRacer Oligo dT Primer. Next, this cDNA was used for PCR using the oligonucleotides of GeneRacer 5′ Primer and P1 primer which hybridized to the coding strand of the *IL28A/B* (Table S1). The resulting PCR products were then used for a second round of PCR using the oligonucleotides GeneRacer 5′ Nested Primer, which represents the DNA equivalent of the 3′ end of the GeneRacer RNA Oligo, and P2, which hybridizes to the coding strand of the *IL-28A/B* 5′ to the P1 hybridization site. For 3′ RACE, the cDNA was subjected to the polymerase chain reaction (PCR) to amplify the 3′ end using a forward gene-specific primer P3 designed from *IL-28A/B* and the GeneRacer 3′ primer provided with the kit. Nested PCR, using the same gene-specific primer and GeneRacer 3′ nested primer, was performed. The PCR product of 5′ and 3′ RACE was cloned into pCR4-TOPO TA vector according to the manufacturer's instructions (Invitrogen). Ten clones were isolated and subjected to automated sequencing (ABI3100, ABI) in our core facility.

Protein expression and purification

Recombinant IL-28B and its mutant were produced by transfecting Free-Style™ 293-F cells (purchased from Invitrogen, Carlsbad, CA) with the expression plasmid, which was grown in 5000 ml of FreeStyle 293 Expression Medium, following the manufacturer's recommendations (Invitrogen, Carlsbad, CA). Cultures were maintained at >90% viability on a shaker plate (Titer Plate Shaker; Lab-Line Instruments, Melrose Park, NJ) moving at 125 rpm in a 37°C incubator with 8% CO_2 and subculturing at a 1:10 ratio upon reaching a density of 2×10^6 cells per ml. Cell density and viability were evaluated with a hemocytometer using 0.4% trypan blue staining. After 96 h, the transfected cell culture was harvested. The supernatant containing the secreted recombinant protein was centrifuged (100×g, 15 min), frozen, and stored at −30°C until use. The 293-F cells supernatant containing the recombinant protein was loaded onto a Ni^{2+} column (Amersham Biosciences) following the manufacturer's directions. Fractions were eluted with 80, 100, 250, and 1000 mM imidazole (in 50 mM Tris, 300 mM NaCl, pH 8.0), and the fraction eluted at 250 mM was pooled and concentrated in an Amicon (10 kDa molecular weight cutoff) to 1 ml (Amersham Biosciences).

Western blot analyses

Purified recombinant protein was loaded onto 12% sodium dodecyl sulfate gels. Proteins were detected with goat anti-IL28 (1:2000) polyclonal antibody (Santa Cruz Biotechnology, Santa Cruz, CA) and the secondary antibody. Proteins were visualized using ECL Plus Western blotting detection reagents (GE Healthcare) and a LuminoImager (LAS-3000; Fujifilm). The band densities were analyzed with the Multi Gauge software (version 3.1; Fujifilm).

IL-28A/B promoter genotyping

Germ-line DNA was extracted from PBMC according to standard methods [14]. Twenty HV samples were genotyped for the dinucleotide insertion/deletion (indel) present in the promoter region of *IL-28A* or *B*, as described below. Twenty ng of genomic DNA were subjected to PCR analysis in 50 µl aliquots containing

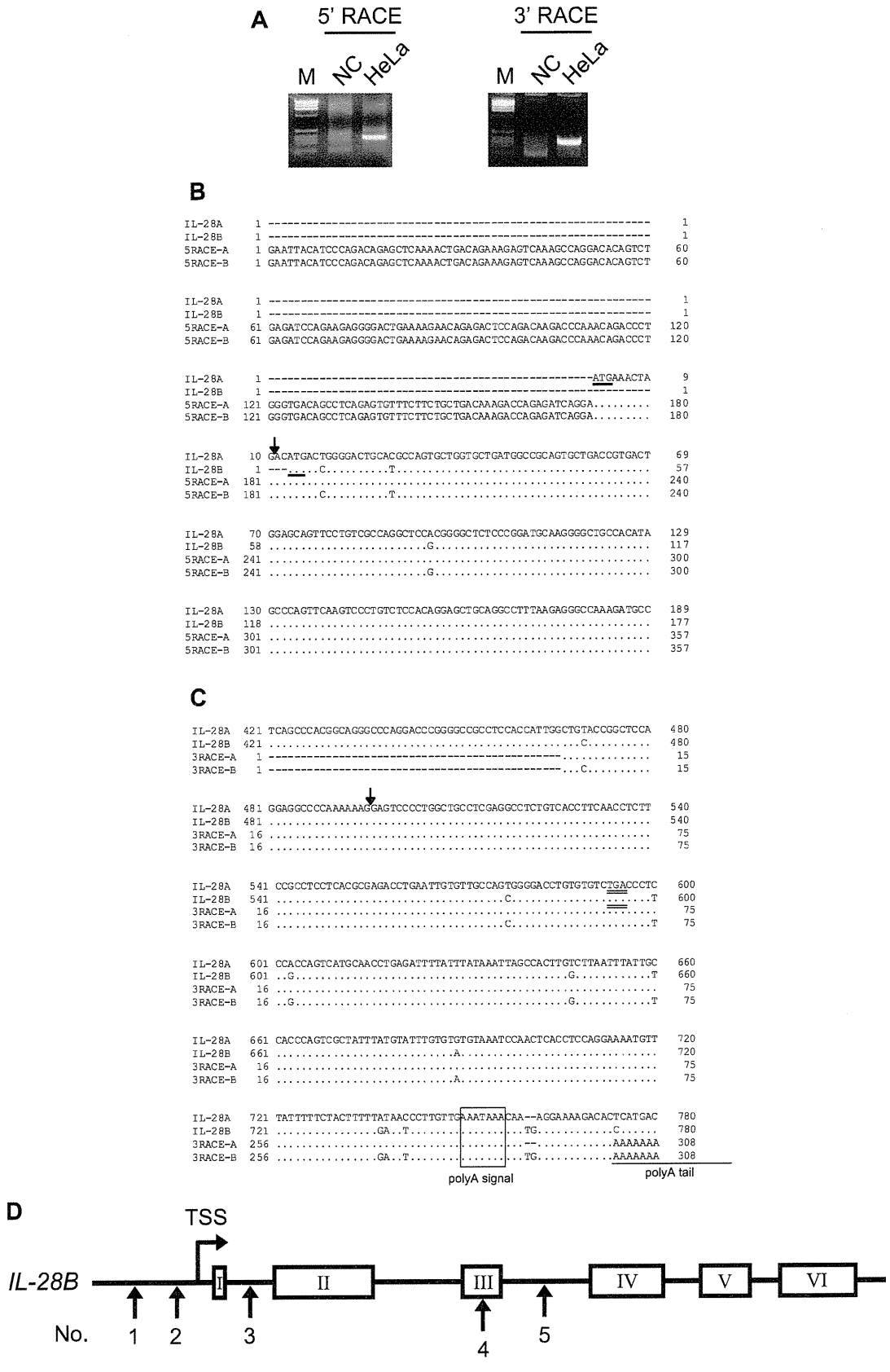
A
5' RACE
3' RACE
M
NC
HeLa
M
NC
HeLa
B
C
polyA signal
polyA tail
D
TSS
IL-28B
I
II
III
IV
V
VI
No.
1
2
3
4
5

Figure 2. The determination of *IL-28B* gene structure and UTR region. *IL-28A/B* cDNA was isolated using a complete cDNA cloning method and the entire sequences were determined using HeLa, MT-2, and Raji call lines and PBMC from healthy volunteers. (A) 5′- and 3′-RACE analyses were used to determine the complete sequence of *IL-28A/B* mRNA after LPS stimulation (3 μg/mL) for 4 h following IFN-α treatment (100 U/mL) for 16 h. A representative example of agarose gel electrophoresis is shown for the non-stimulated control (NC). PCR products were inserted into the cloning vector and 6 clones of 5′- and 3′-RACE were analyzed by sequencing. (B) mRNA sequences of the 5′ terminal region were aligned using CCDS retrieved from NCBI and RACE data of *IL-28A/B*. The upper two sequences are reference sequences from the NCBI CCDS and the lower two are representative sequences of *IL-28A* and *28B* obtained from 5′-RACE. The underlined triplet indicates the start codon of each gene and arrow shows the splice junctions. (C) mRNA sequences of the 3′ terminal region were aligned using CCDS retrieved from NCBI and RACE data from *IL-28A/B*. The double-underlined triplet indicates the stop codon of each gene and arrows show the splice junctions. The polyA signal and representative site of polyadenylation also are shown. (D) The derived gene structure of the *IL-28B* is shown with the significant SNPs. The location of SNP No. 3 was changed from the regulatory to an intron region. The transcription start site (TSS) is found behind SNP No. 2.
doi:10.1371/journal.pone.0026620.g002

20 pmol of each primer, 5×PrimeSTAR GXL Buffer, 2.5 mM each deoxynucleotide triphosphates, and 1.25 units of PrimeStar GXL DNA polymerase (TAKARA Bio Inc, Tokyo, Japan). The primer pair, G1 and G2 (listed in Table S1), was used for the simultaneous amplification of the *IL-28A* and *28B* regulatory regions. The PCR conditions were as follows: 30 cycles of 10 s at 98°C, and 120 s at 68°C in addition of initial denaturation at 98°C for 5 min and a final extension at 68°C for 10 min. To separate the *IL-28A* amplicon from that of *IL-28B*, 10 μl of PCR products were analyzed using agarose gel electrophoresis and extracted with QIAquick Gel Extraction Kit (Qiagen). Each extracted product was analyzed by direct sequencing using Seq1 and Seq2 primers (Table S1). For further testing of the TA repeat, heterozygous samples were cloned into the pGEM-Teasy vector to count the number of TA repeats in each allele. Six clones were isolated and subjected to sequencing analysis using the primers described above.

Reporter assay

Luciferase assays of recombinant protein were performed using Dual-Glo Luciferase reporter assay system (Promega, Fitchburg, WI). In toll-like receptor (TLR)-stimulated experiments Raji cells were transfected and left for 16 h with 100 U/mL of IFN-α, then were exposed to LPS (3 μg/ml) for 4 h before harvesting. For assessments of recombinant protein, HeLa cells were transfected with pISRE-Luc and pGL4.74, and were harvested 24 h after IFN-α or λ treatment. The chemiluminescence was measured by SpectraMax L (Molecular Devices, Sunnyvale, CA). Firefly luciferase activity was normalized to Renilla activity to adjust for transfection efficiency.

Real-time PCR detection

Jurkat cells were transfected with the *IL-28B* expression vector harboring a FLAG sequence derived from the natural promoter (pdCMV/MA, mi, or AS). To induce IL-28B expression, TLR and IFN-α stimulation was given as described above. FLAG and glyceraldehyde-3-phosphate dehydrogenase (GAPDH) mRNA expression were measured using a real-time PCR performed on ABI Prism 7700 sequence detection system (Applied Biosystems) using primer sets (Table S1) after total RNA extraction and reverse transcription (RT) using an RT kit and TaqMan Universal PCR master mix (both Applied Biosystems), according to the manufacturer's manual. Relative gene expression was calculated as a fold induction compared to the control. Data were analyzed by the 2[-Delta Delta C(t)] method using Sequence Detector version 1.7 software (Applied Biosystems) [18] and were normalized using human GAPDH. A standard curve was prepared by serial 10-fold dilutions of human cDNA or FLAG plasmid. The curve was linear over 7 logs with a 0.998 correlation coefficient.

Statistical Analysis

Statistical analyses were conducted by using SPSS software package (SPSS 18J, SPSS, Chicago, IL) and Microsoft Excel 2007 (Microsoft co., Redmond, WA). Discrete variables were evaluated by Fisher's exact probability test. The P values were calculated by two-tailed student's t-tests for continuous data and chi-square test for categorical data, and those of less than 0.05 were considered as statistically significant.

Results

The identification of IL-28B gene structure

To define the human *IL-28A* or *IL-28B* gene structure, 5′-RACE and 3′-RACE were performed on total extracted RNA from HeLa, MT-2, Raji, HuH7 cells, and PBMCs from healthy volunteers (Fig. 2A). The sequences obtained matched the genomic contig of AC011445, which contains the sequence of *IL-28A* and *IL-28B* in forward and reverse orientations, respectively. All intron/exon junctions conformed to the canonical GT-AG rule. After stimulation of cells with LPS (3 μg/ml) for 4 h following IFN-α treatment (100 U/mL) for 16 h, *IL-28A/B* transcripts were detected in RACE experiments, but these were not detected in unstimulated cells. The representative TSSs are shown in Fig. 2B and showed little variation among cloned mRNA transcripts. The same 3′-UTR fragment also was detected without any intron in the 3′-RACE experiments (Fig. 2C). A polyadenylation signal (AAAUAAA), located in the 3′-UTR, was found upstream of the polyadenylation site in all samples. All sequences from the transcripts were aligned on the 5′-UTR, the six exons, and the 3′-UTR region of *IL-28A/B*. No different mRNA transcripts of *IL-28A/B* were found in our experiment. Taken together, the *IL-28B* gene structure comprised six exons (see Fig. 2D), and the location of SNP no. 3 (rs28416813) is in an intron, rather than a regulatory region (Table 1).

The effect of regulatory SNPs on promoter activity

Because the TSS was upstream of the position described in previous reports (Fig. 2), two rSNPs (rs72258881 and rs4803219) in the regulatory region were more specifically located in the TSS. A luciferase reporter approach was used to assess the effects of the two rSNPs on promoter activity. Luciferase vectors harboring the rSNPs were constructed and used for transfections (Fig. 3A). The promoter activities of the constructs were measured after stimulation with LPS (3 μg/ml) for 4 h following IFN-α treatment (100 U/mL) for 16 h. The transcriptional activity of constructions harboring the $(TA)_{11}$ mutation was reduced (Fig. 3B). Substitution in the rSNP (rs4803219) showed little effect on the transcriptional activity, whereas the number of TA repeats could be responsible for the putative region controlling basal transcription. To confirm the transcriptional activity, Jurkat cells were transfected with full length constructs expressing the FLAG sequence under the control of the natural promoter (Fig. 3C). To avoid the detection of endogenous mRNA, the mRNA with the FLAG sequence was specifically detected by real time PCR using the FLAG primer. The constructs harboring $(TA)_{11}$ yielded lower expression levels

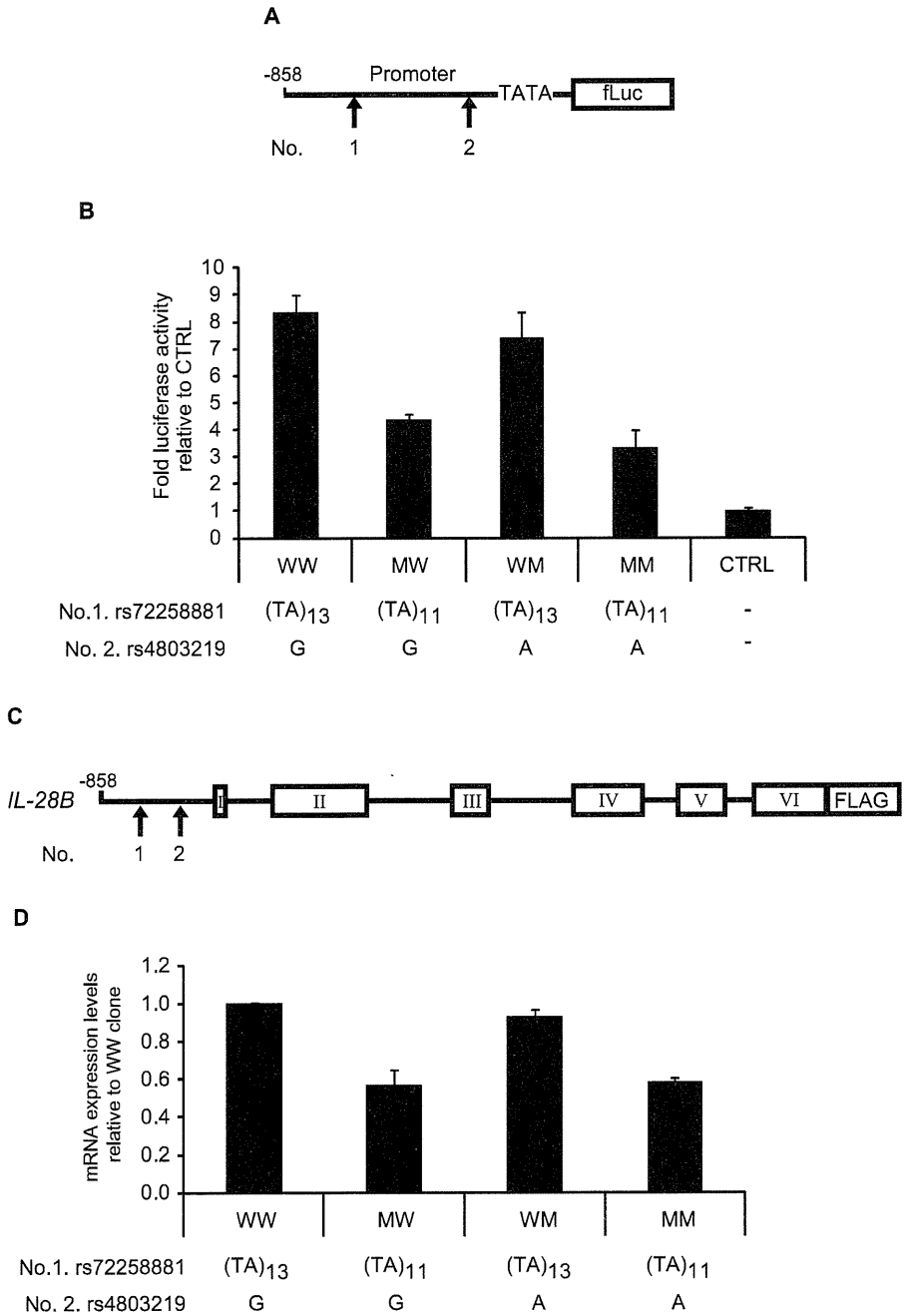

Figure 3. Transcriptional activity of the *IL-28B* promoter region compared between major and minor alleles. (A) The pGL4 reporter plasmid was constructed by subcloning the *IL-28B* promoter subfragment (nt −858 to +30). The combinations of two regulatory SNPs (rs72258881 or rs4803219) were introduced into the pGL4 vector (pGL4/WW, MW, WM, and MM). (B) Raji cells were co-transfected with pGL4 plasmids (0.05 g), and pGL4.74 control plasmid (0.05 g), and tested for firefly as well as renilla luciferase after LPS stimulation (3 μg/mL) for 4 h following IFN-α treatment (100 U/mL) for 16 h. These cells were seeded in a 96-well plate at 10^4 cells/well. The luciferase activities were normalized with renilla activities and data are presented as fold induction from activation of control vector. Bars indicate the means ± SD of triplicate determinations and the results are from one of three experiments. Statistical analyses are shown in table S2 to avoid complication. (C) For real-time PCR, the combinations of two regulatory SNPs (rs72258881 or rs4803219) were introduced into the pdCMV vector harboring a FLAG sequence (pdCMV/WW, MW, WM, and MM). (D) Jurkat cells were co-transfected with pdCMV plasmids (0.05 μg) and secreted alkaline phosphatase (SEAP) control plasmid (0.05 μg) and the expression levels were quantified using specific primer after LPS and IFN-α stimulation. The FLAG expression levels were normalized with SEAP activities and GAPDH as described in method section. Data are presented as fold induction from expression levels of pdCMV/WW. Bars indicate the means ± SD of triplicate determinations and the results are from one of three experiments. Statistical analyses are shown in table S3 to avoid complication.

doi:10.1371/journal.pone.0026620.g003

after IFN-α and LPS stimulation (Fig. 3D), suggesting that the length of TA repeat in the regulatory region of *IL-28B* could affect the regulation of *IL-28B* transcription.

Two intron SNPs located near the branch site of splicing

To determine the effect of the two iSNPs on pre-mRNA splicing, HeLa cells were transfected with wild type (WT), a construct with a double mutation of the iSNPs (d-iSNPs), or an antisense (AS) plasmid driven by the CMV promoter (Fig. 4A). The construct providing antisense transcription controlled by the CMV promoter was used to control for splicing defects (AS). Transcripts were analyzed by RT-PCR using primers in exon 1–2, 3–4, and 4–5. The RNA isolated from the WT and d-iSNPs yielded a single band using the three primer pairs. In contrast, longer amplicons were generated in cells expressing the antisense construct (Fig. 4B). The PCR products were sequenced to confirm the origin of the aberrant splicing events derived from the antisense construct (data not shown). The sequence analyses confirmed that PCR products from the WT and d-iSNPs were generated by normal splicing, suggesting that these two intron SNPs resulted in no splicing defects under these conditions.

No effect of nonsynonymous SNPs on IL-28B function

A nonsynonymous SNPs (rs8103142) located in the 3rd exon (Table 1 and Fig. 2D) led to the amino acid substitution $K^{74}R$ (Fig. 5A). Interestingly, the amino acid at this position is almost always arginine in homologous mammalian IFN-λs (e.g. human IL-28A, mouse IL-28A/B, and rhesus IL-28A/B). Then, the $K^{74}R$ substitution was expected to change IL-28B activity. The purified recombinant IL-28B protein (wild type) and the variant (ns-mut) were recognized by anti-IL-28B polyclonal antibody in a western blot assay (Fig. 5B). Based on spectrophotometric measurement of the protein concentration of the eluted fraction, it was calculated that at least 360 μg/mL of purified recombinant IL-28B protein (wild type and ns-mut) was obtained after purification. Flow-through liquid without recombinant protein was provided in the column preparing the sample of pcDNA3.1/AS (Fig. 5B). Molecular processing of IL-28B protein was confirmed to determine the precise N-terminal amino acid by peptide sequencer as the processing site of signal peptide was predicted by computer simulation (http://www.uniprot.org/uniprot/Q8IZI9). Then, the N-terminal sequence, VPVAR, was obtained (data not shown), suggesting that the simulation data was consistent with the form of physiological protein.

To evaluate the effect of nsSNPs on ISRE activity, three hepatoma cell lines (HuH7, HepG2, and HuSE2) expressing IL-28R1 and IL-10R2 were transfected with pISRE-Luc and pGL4.74. These recombinant proteins were added to the supernatant (5 ng/mL each). As shown in Fig. 5C, ISRE activity of the ns-mut protein was similar to that of wild type protein in each cell line. IFN-α (100 U/mL), as a positive control of ISRE activity, showed a strong ISRE activity. These results suggested that the nonsynonymous mutation of rs8103142 did not affect IL-28B activity *in vitro*.

The genetic variation of TA repeats at the upstream of *IL-28B*

The reference sequence (RefSeq) of the human genome in the international database registers the TA repeat SNPs, rs72284729 or rs72258881, in the regulatory regions of *IL-28A* and *IL-28B*, respectively. The registered basal number of $(TA)_n$ is 8 in the regulatory region of *IL-28A* on the plus strand, whereas that of *IL-28B* is 13 on the minus strand encoding the gene (Table 2). From 20 Japanese healthy volunteers, genomic DNA was extracted to determine the actual $(TA)_n$ number located in the region of *IL-28A* or *IL-28B* by direct sequencing and, when direct sequencing chromatographs of $(TA)_n$ heterozygotes showed mixed patterns from the end of the TA repeat (Fig. S4), the mixed samples were subjected to cloning analysis. Interestingly, the $(TA)_n$ number in *IL-28A* was consistently different from dbSNP data, whereas that of *IL-28B* showed varying numbers along with SNPs data. The $(TA)_n$ range of *IL-28B* was from 10 to 18, and the most prevalent genotype was 12/12 (75%) in healthy Japanese volunteers.

To determine the functional significance of the TA indel, the regulatory region from −858 bp to +30 bp modifying the $(TA)_n$ number was cloned into the pGL4 reporter vector, transfected into HeLa cells, and assessed for firefly luciferase reporter gene

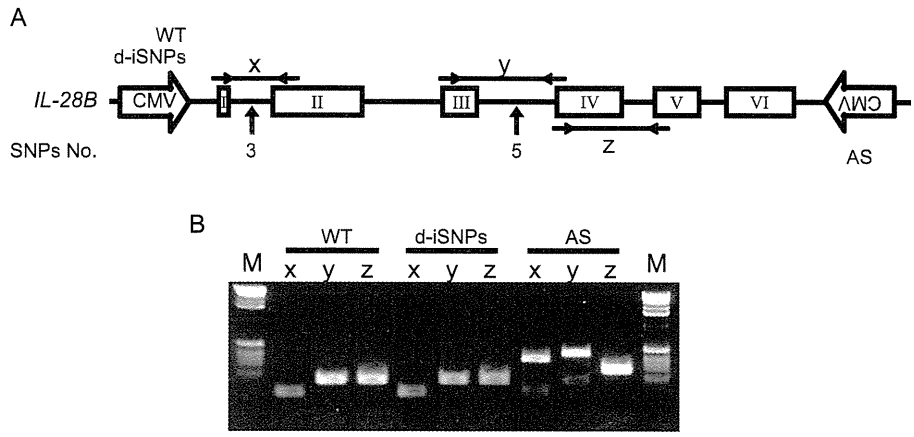

Figure 4. The determination of intron SNPs located near the branch site of splicing. (A) The expression plasmid of WT, d-iSNPs, or antisense (AS) derived from the CMV promoter was transfected into HeLa cells. Schematic of the WT, d-iSNPs, or AS used in the transfection experiments. PCR primers were designed to amplify products between exons. The effect of No. 3 and 5 SNPs (rs28416813 or rs11881222) on splicing were examined by amplicons x and y, respectively. The amplicon z was used for a splicing control. (B) Isolated RNAs were amplified by RT-PCR. The amplified products were checked by 2% agarose gel electrophoresis. The bands from the AS plasmid transcribing antisense represented abnormal splicing of mRNA as a control. Results shown are representative of three independent experiments.
doi:10.1371/journal.pone.0026620.g004